Proceedings of the 38th International Conference on Ocean, Offshore and Arctic Engineering
OMAE2019
June 9-14, 2019, Glasgow, Scotland

OMAE2019-96347

HYDRAULIC BEHAVIOR IN CASED AND OPEN HOLE SECTIONS IN HIGHLY DEVIATED WELLBORES

Jan David Ytrehus[1], Bjørnar Lund, Ali Taghipour, Birgitte Ruud Kosberg
SINTEF
Trondheim, Norway

Luca Carazza
Aker BP
Stavanger, Norway

Knud Richard Gyland
Schlumberger, MI-SWACO
Stavanger, Norway

Arild Saasen
University of Stavanger
Stavanger, Norway

ABSTRACT

In this paper we present results from flow loop experiments with an oil-based drilling fluid with micronized barite as weight materials. The use of micronized barite allows using lower viscosity drilling fluid, providing non-laminar flow, which is advantageous for particle transport in near-horizontal sections. While transition to turbulence and turbulent flow of non-Newtonian fluids has been well studied both theoretically and experimentally, there are very few published results on the effect of wellbore wall properties on flow regime transition and turbulence. This is relevant because horizontal sections are often open-hole with less well-defined surfaces than a steel casing surface. We have conducted a series of flow experiments with and without cuttings size particles in a 10 m long annular test section using steel and concrete material to represent the wellbore wall of a cased and open hole section. In both cases the annulus was formed by a freely rotating steel pipe of 2" outer diameter inside a 4" diameter wellbore. Experiments were conducted at 48°, 60° and 90° wellbore inclination from vertical. The two materials result in different hydraulic behaviour without particles with stronger turbulence when using concrete wellbore wall material than when using steel casing. While there is negligible difference at low flow rates, at 0.8 m/s and below, there is an increasing difference as the flow rate increases and becomes transitional to turbulence. Hole cleaning is found to differ dependent on the wall material. However, the effect on hole cleaning is less clear than for the pressure loss.

INTRODUCTION

Most Norwegian offshore wells have a significant deviated reservoir section. These wells must be drilled and completed in an optimal manner to reduce drill time and operational risks, and to optimise functionality. To plan these drilling operations, it is necessary to use good and accurate engineering models in all drilling perspectives.

Drilling fluid hydraulic models go beyond the limits for analytic calculations because of hydrodynamic stability issues and turbulence. Empirical models are required to close the hydrodynamic set of equations. These models are normally developed from small scale laboratory experiments. Since laboratory work with real drilling fluids can be complicated because of HSE issues like waste handling and exposure to saline fluids, emulsifiers and hydrocarbons, most hydraulic models are developed based on tests with simple water-based fluids. With the exception where some simple bentonite muds are used, hole cleaning with oil based drilling fluids is different than hole cleaning obtained with proper water based fluids [1], [2] possibly partly due to presence of colloidal

[1] Contact author: JanDavid.Ytrehus@sintef.no

effects and normal stress differences in the water based drilling fluid [3].

According to field practice, oil based drilling fluids are anticipated to be superior to water based drilling fluids when it comes to hole cleaning, even if the fluid properties are equal as measured in accordance with API specifications. This anticipation was later verified in medium scale laboratory experiments [1], [2].

In a comprehensive article, Li and Luft [4] reviewed the theoretical analyses for hole cleaning. Later, they expanded their work to include experimental studies [5]. A recent review on hole cleaning in horizontal sections were conducted by Busahmin et al. [6]. This review included an analysis of the effects of yield point, plastic viscosity as determined following API specifications [7]. However, the yield point and the plastic viscosity used in this specification are by far too high to be representative in determination of the viscosity parameters relevant in hole cleaning [1].

So far, little focus has been given to investigations about differences in hole cleaning between open hole or cased hole. Historically, one of the first severe hole cleaning incidents was observed at certain well angles in the cased hole at a major North Sea field. Whether the hole cleaning would have been different in similar open hole sections is unknown. The scope of the current article is to present data showing the differences between hole cleaning in open and cased hole.

Recent investigators have evaluated hole cleaning with numerical simulators [8], [9], [10], [11]. However, none of these simulations have been able to model the differences between the open hole or cased hole surfaces. For such cases experiments provide significant value to the analysis [10], [12].

EXPERIMENTAL

The experiments are conducted in the medium size flow loop shown in FIGURE 1. This is constructed with the possibility of free whirling motion of the drill string with simultaneous drill string rotation. The entire test section is mounted on a steel frame that can be tilted from 90° (horizontal) to an inclination of 48°. The annular dimensions of the flow loop allow for comparing results with field data. The circulation system is closed such that field fluids, both oil-based and water-based, can be used. The closed circulation system includes a particle handling system where cuttings are introduced from a cuttings feeder tank before being transported through the flow loop by the pumped flow into a reception tank. The current flow loop experiments were conducted both without particles and with quartz sand particles with size in the range from 0.9mm to 1.6mm. The sand was delivered from Dansand A/S.

The experimental setup, shown in FIGURE 2, consists of the following main components

1. Drilling fluid storage tank
2. Sand injector unit
3. Liquid slurry pump
4. Density and flow meter
5. Test section with pressure transducers
6. Sand separator
7. Sand storage system and fluid to return storage tank

The test section itself is 10 m long. It consists of an outer support pipe, into which either a cylindrical steel housing or a continuous series of hollow cement inserts are placed to represent the cased hole or open wellbore wall, respectively. A transparent part of the housing is placed in the middle of the test section for visual inspection of the flow.

FIGURE 1. PICTURE OF THE FLOW LOOP TEST SECTION.

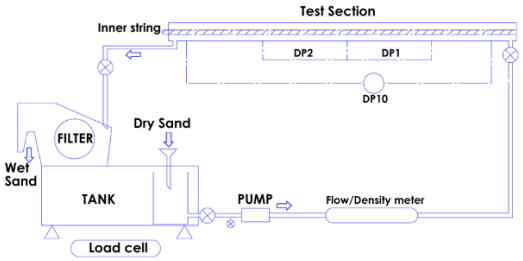

FIGURE 2. SKETCH OF THE FLOW LOOP.

The cased wellbore was constructed from steel pipes giving an outer annular diameter of D_o = 100 mm. For the open hole representation replaceable hollow cylindrical sections of cement with similar outer annular diameter was applied.

A steel rod of D_i = 50 mm diameter inside the wellbore represents the drill string and defining the inner diameter of the annular test section. This rod is connected to a drive motor at one end. The other end is attached to a load cell using universal flexible joints allowing free whirling (lateral) motion within the constraints of the wellbore. Due to gravity the drill string is fully eccentric. Movement in the axial direction is constrained while the free whirling capability allows it to climb parts of the wellbore wall for high rotation rates.

The instrumentation consists of a Coriolis flow meter and differential pressure (DP) transducers

along the test rig connected to the logging system. One DP cell (DP1) measured differential pressure between pressure ports located at positions 4 m and 6 m from the inlet, and another DP cell (DP2) measured between positions 6 m and 8 m from the inlet. DP2 is used for the pressure drops reported here.

The particle mass rate is controlled by the frequency of the sand injector based on calibration tests. Cuttings injection rates are 43 g/s, representing a rate of penetration (ROP) of 8 m/hr for the hole sizes applied in the test setup. Due to the opacity of the fluid, visual measurement of the bed height is not possible, and the average bed height was calculated from weight measurements using load cells under the fluid processing system. For transparent model fluids visual inspection is possible [13].

FLUID AND VISCOSITY PARAMETERS

The fluid applied in all tests reported here is an oil-based drilling fluid commonly used on the NCS. Similar fluids have frequently been used for drilling extended reach wells, including for example wells at the Hibernia field offshore Newfoundland [14]. The fluid is constructed from standard OBM components except from the weight material that is a micronized barite slurry of 2.3 SG. The base oil is non-aromatic. Rheological properties are measured with Anton Paar rheometer in addition to the standard API tests with Fann 35 viscometer. The flow curve data are fitted to the Herschel-Bulkley model and plotted in FIGURE 3.

The flow experiments were conducted during a four-month period, where the rheological measurements were conducted frequently in order to control the properties of the fluid. The average density, as measured with inline Coriolis flowmeter, was 1430 kg/m3, decreasing from 1450 kg/m3 at the start of the experiments to 1410 kg/m3 at the end of the experiments. The drilling fluid viscosity is adequately described using the Herschel-Bulkley model. The viscous parameters are summarized in Table 1, both for the traditional description (Equation 1) and for the Saasen and Ytrehus [15] description (Equation 2). The shear stress is given as

$$\tau = \tau_y + k\dot{\gamma}^n \qquad (1)$$

where τ_y is the yield stress, k the consistency parameter and n the curvature exponent, or as

$$\tau = \tau_y + \tau_s \left(\frac{\dot{\gamma}}{\dot{\gamma}_s}\right)^n \qquad (2)$$

where the surplus stress, $\tau_s = \tau - \tau_y$ is measured at a relevant shear rate of $\dot{\gamma}_s$.

Flow curves taken in May and August show very little change in fluid properties over this period. The Herschel-Bulkley parameters shown in Table 1 are based on measurements from August 2017. In calculation of the fluid parameters, the yield stress τ_y was determined by extrapolating the flow curve down to zero shear rate since the yield stress is a material property. Then the consistency index k and the flow behavior index n for the old model were determined by fitting the Herschel-Bulkley model (1) to the flow curve based on the shear rates 0 – 300 1/s. For the new Herschel-Bulkley approach (2) a surplus stress was calculated from a shear stress reading at the shear rate of 201 1/s. The additional surplus stress was applied together with the measurement at 101 1/s to calculate the behavior index n. The motivation for introducing this new model is to have a formulation of Herschel-Bulkley with only independent parameters making the tabulated values suitable for digitalization. The consistency index k of the old formulation (1) is not independent of the behavior index n.

The investigated fluid was a field applied drilling fluid with properties specially designed for drilling extended reach wells with low dynamic pressure drop (ECD).

TABLE 1. SUMMARY OF HERSCHEL-BULKLEY PARAMETERS AS CALCULATED FROM THE FLOW CURVES AT 25 C AT 201 1/S SHOWN IN FIGURE 3. *n* IS CALCULATED AT 101 1/S FOR NEW MODEL

Model	τ_y [Pa]	k [Pa*s^n]	τ_s [Pa]	τ_{201} [Pa]	*n*
Old	0.2	0.0548	*4.40*	*4.60*	0.8269
New	0.2	*0.0591*	4.35	4.55	0.8107

The flow curve obtained from measurements using an Anton Paar MCR102 Rheometer, at 25°C (typical fluid temperature in flow loop), is presented in FIGURE 3

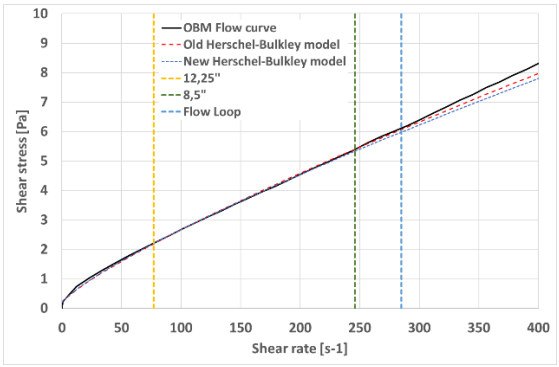

FIGURE 3. PLOT OF FLOW CURVE FOR THE APPLIED OBM AT 25°C AND CORRESPONDING HERSCHEL-BULKLEY PLOTS. SHEAR RATES FOR 8,5" AND 12.25" SECTIONS WITH 5,5" DRILL PIPE ARE BELOW THE CORRESPONDING LINES FOR OPERATIONALLY APPLIED PUMP RATES. THE SHEAR RATE LIMIT IN THE FLOW LOOP (2" PIPE IN 4" HOLE) WITH THE APPLIED TEST PARAMETERS IS ALSO PLOTTED.

FLOW LOOP RESULTS

In FIGURE 4 we have plotted the pressure gradient versus flow rate for hydraulics experiments with horizontal test section. Flow rates are reported in terms of average liquid flow velocity in full area annulus. The experimental data are based on the DP2 pressure transducer where the flow is assumed

to be close to fully developed. Experience has also shown that data from this sensor is closer to the theoretical values for fully developed flow. The calculations are done with the semi-empirical model by Founargiotakis [15] and have been corrected for eccentricity by using the correlations of Haciislamoglu et al. for laminar [16] and turbulent [17] regimes, respectively., These model results agree well with the experimental results for cased hole through the entire data range. Note that while the correlations by Haciislamoglu et al. were developed for power-law fluids, there is no significant effect of using the generalized flow behaviour index n' (see eq. 14 in [15]) instead of n with our data. Kelessidis et al. [18] also applied this correlation to Herschel-Bulkley fluids, using the flow behaviour index n from the HB model,

At the lowest flow rate there is no difference in pressure gradient between cased hole and open hole test results. However, at all higher flow rates the open hole tests give a larger pressure gradient than the cased hole test, and the difference increases with flow rate. Also, the cased hole data agree well with the model results for all flow rates from laminar to turbulent. The model predicts a transitional region between laminar and turbulent flow from 0.8 m/s to about 1.1 m/s. This is consistent with the cased hole data, although it is not possible to identify the start and end of the transitional region from the experiments due to the limited number of data points. It seems that the transitional region (to turbulence) starts at lower flow rates for the open hole than for the cased hole section.

The wall roughness is higher in the open hole configuration compared with the cased section. In principle this is the only relevant parameter difference between the two test sets. Note that wall roughness is not included in the model [15].

Thus, the data indicate that there is a transition from laminar flow starting somewhere between 0.7 and 0.9 m/s, which corresponds to a Reynolds number of approximately 2500. Here the Reynolds number is defined as

$$Re = \frac{\rho_l D_{hl} U}{\mu_{wall}} \qquad (3)$$

where ρ_l is the liquid density, D_{hl} is the hydraulic diameter, U is the average liquid velocity and μ_{wall} is the viscosity at the wall as calculated using the laminar model by Founargiotakis [15].

An observation from FIGURE 5 is that the pressure drop is higher in an open hole configuration than in a cased hole configuration also when cuttings are present in the flow. This supports the observations in the hydraulic tests without cuttings. Both these observations are done in horizontal test section. From the tests without sand particles, shown in FIGURE 4, it can be observed that the pressure loss for lower flow rates around 0.5 m/s approaches that of the cased hole. This is anticipated to be caused by existence of laminar flow in the entire annulus. For the higher flow rates, where at least part of the cross-sectional flow is non-laminar, the higher roughness of the open hole wall should create a higher turbulence intensity and thus a larger pressure loss. This hypothesis is supported by the experimental observations. Since experiments in cased hole are not conducted with cuttings at velocities below 0.7 m/s it is not possible to compare pressure drops at 0.5 m/s for cased and open hole configurations and validate if the similar trend is valid also with cuttings.

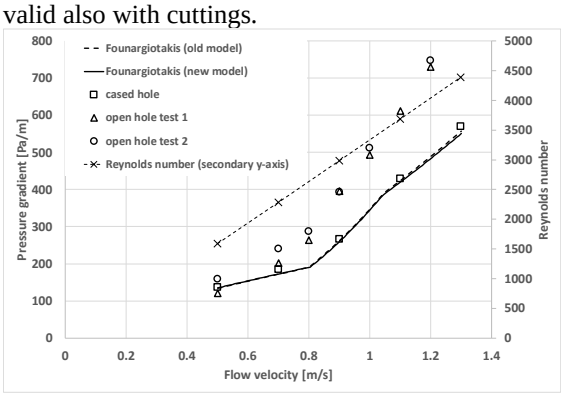

FIGURE 4. PLOT OF MEASURED AND CALCULATED PRESSURE GRADIENT FOR LOW ECD OBM IN HORIZONTAL, ECCENTRIC CASED AND OPEN HOLE ANNULUS WITHOUT ROTATION AND WITHOUT CUTTINGS.

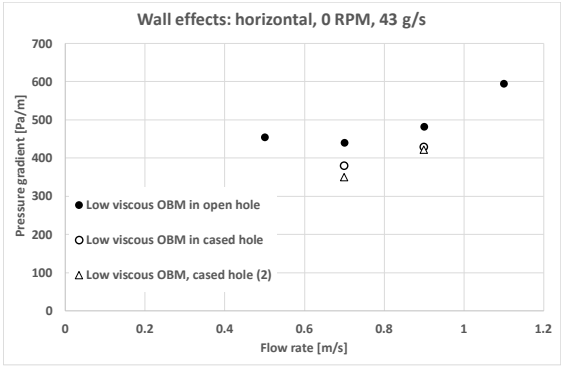

FIGURE 5. PLOT OF MEASURED PRESSURE GRADIENT FOR LOW ECD OBM IN HORIZONTAL, ECCENTRIC CASED AND OPEN HOLE ANNULUS WITHOUT ROTATION AND WITH CUTTINGS INJECTION RATE CORRESPONDING TO 8 M/HR ROP.

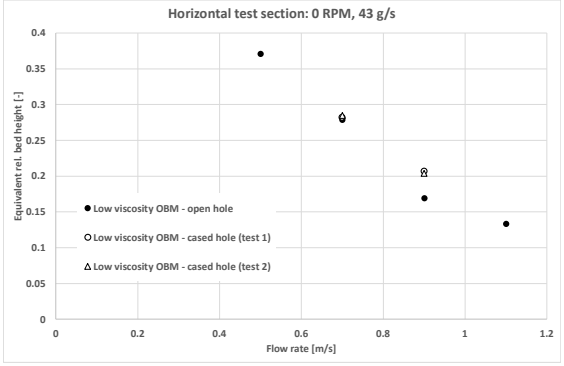

FIGURE 6. SAND BED HEIGHT PLOTTED FOR LOW ECD OBM AS FUNCTION OF ANNULAR VELOCITY WITHOUT DRILL STRING ROTATION AT HORIZONTAL CONDITIONS. SAND INJECTION RATE IS 43 G/S. TEST 2 IS A REPETITION OF TEST 1.

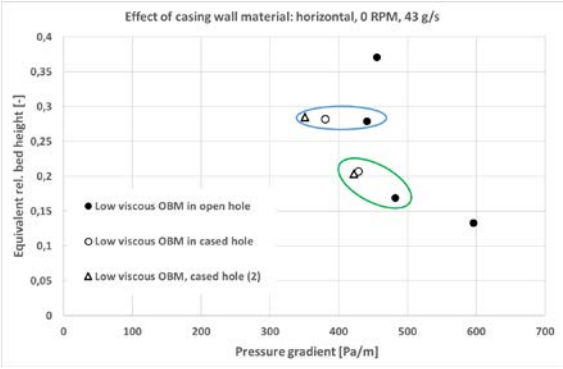

FIGURE 7. SAND BED HEIGHT PLOTTED FOR LOW ECD OBM AS FUNCTION OF PRESSURE GRADIENT WITHOUT DRILL STRING ROTATION AT HORIZONTAL CONDITIONS. SAND INJECTION RATE IS 43 G/S. TEST 2 IS A REPETITION OF TEST. RESULTS FOR LOCAL ANNULAR VELOCITY 0.7 M/S ARE CIRCLED IN THE BLUE ELLIPSE AND 0.9 M/S ARE IN THE GREEN ELLIPSE.

The cuttings bed height in horizontal section, plotted in FIGURE 6 and FIGURE 7, is observed to be lower in an open hole configuration than in the cased section at a flow rate of 0.9 m/s, while there is no difference at 0.7 m/s. Thus, it appears that the bed height in the open hole section becomes lower than in the cased hole section above a critical flow rate, somewhere between 0.7 m/s and 0.9 m/s. This difference between cased hole and open hole can possibly be explained by an earlier transition to turbulence and stronger turbulent energy dissipation for the open hole than for the cased hole. Also, it is expected that the effect of turbulence on bed height starts at a higher flow rate than indicated by FIGURE 4 due to the non-uniformity of the flow across the annulus, as illustrated in FIGURE 8. Turbulence will first be generated in the widest part of the annulus. This is illustrated in FIGURE 8 where it can be observed that a fairly significant cuttings bed can exist without being affected by velocities causing flow to leave laminar area [19]. When the flow velocity increases the cross section dominated by turbulence will also increase. This increased turbulence increases the pressure loss and, hence, the shear stress onto the cuttings bed. When this turbulent behavior becomes sufficient the cuttings bed is affected and reduced. The increased flow area will cause the pressure drop to decrease until the shear stress on the cuttings bed again gives a dynamic equilibrium between particle deposition and entrainment. Although detailed information about the velocity field above the cuttings bed is not available from the present experiments, the hypothesis is that stronger turbulent activity at intermediate flow rates for open hole gives increased particle entrainment (relative to cased hole) and thus shifts the equilibrium towards lower bed height.

Based on the results plotted in FIGURE 7, it may appear to be beneficial to have a flow velocity of 0.9 m/s in open hole when no rotation is applied for this fluid. A higher flow rate will cause the pressure drop to increase significantly with only small reduction in bed height. Conversely, increasing the flow rates from 0.5 up to 0.9 m/s does not create much increase in pressure drop, while the bed height is significantly reduced.

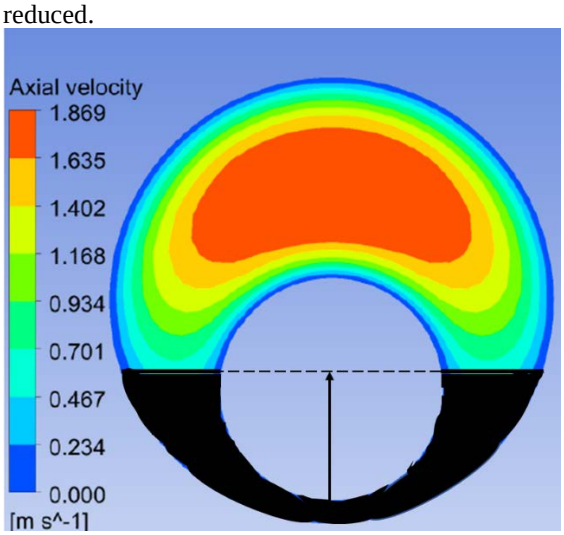

FIGURE 8. ILLUSTRATIVE PLOT OF AN ANNULAR SECTION WITH AVERAGE VELOCITY 1 M/S. CUTTINGS BED IN CROSS SECTIONAL AREA IS ILLUSTRATED IN BLACK.

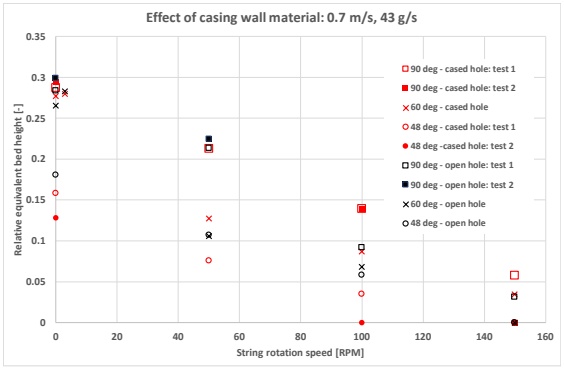

FIGURE 9. SAND BED HEIGHT FOR ANNULAR VELOCITY OF 0.7 M/S AS FUNCTION OF DRILL STRING ROTATION AT THREE INCLINATIONS FOR CASED AND OPEN HOLE CONDITIONS. SAND INJECTION RATE IS 43 G/S. TEST 2 IS A REPETITION OF TEST 1.

FIGURE 9 and FIGURE 10 show the effect of drill string rotation and wellbore inclination on sand bed thickness at flow rates of 0.7 m/s and 0.9 m/s, respectively. The bed thickness is shown for the well angles 48º, 60º and 90º (horizontal). The sand injection rate was 43 g/s, which corresponds to the particle addition from drilling at an ROP of 8 m/hr.

The following observations are made based on the data presented in the figures. a) Reproducibility is good for horizontal and 60 degrees, but poorer at 48 degrees. The latter could be due to the complex flow pattern which is expected to be present when the inclination is below the avalanche angle. b) For given flow rate, inclination and well type (open or cased hole) the bed height decreases with increasing string rotation speed (RPM), except for a small increase from 0 to 3 RPM (FIGURE 9). c) The effect

of inclination is more complex and depends on both flow rate, RPM and possibly hole type, as discussed below. d) Open hole gives smaller bed height than cased hole at 0.9 m/s in horizontal well for all RPM. For the other inclinations and at 0.7 m/s there is no significant difference, or no clear trend found.

Returning to the effect of inclination, it is noted that at 0.7 m/s (FIGURE 9), and at 0 RPM, there is no difference in bed height between horizontal and 60 degrees, whereas bed height decreases between 60 and 48 degrees. At 50 RPM the bed heights at 60 and 48 degrees are similar and significantly lower than for horizontal well. This applies for both well types. At 0.9 m/s (FIGURE 10), bed height appears to be decreasing continuously with decreasing inclination for both hole types at 0 RPM, while the effect of inclination is more complex for rotating pipe. It thus appears that, at least within a range of flow rates, there is a critical well inclination such that bed height is insensitive to inclinations above the critical angle but decreases with decreasing angles below the critical angle. At 0 RPM and 0.7 m/s this critical angle is then between 60 and 48 degrees for the present experiments, while at 50 RPM the critical angle is between 90 and 60 degrees.

The observed effect of wellbore inclination on bed height is contrary to most published results. The following hypothesis is given. When the inclination is below a critical value, the bed becomes unstable. While this instability may cause backsliding of the lower part of the bed, it may also enhance the entrainment of particles from the bed layer to the suspended layer. Since the test section is much shorter than a well, suspended particles may be transported out before they are allowed to resettle again. String rotation may trigger bed sliding at inclinations closer to horizontal, by reducing the effective axial friction force between bed and wellbore wall.

These observed critical wellbore angles were reported in [20] for cased hole tests, and the open hole tests show similar trends. This supports and validates the previous findings.

The difference in bed height between open hole and cased hole in horizontal well observed at 0.9 m/s can be explained by the differences in turbulent conditions as discussed above. This hypothesis is also supported by the difference in bed height between open hole and cased hole in horizontal well at 0.7 m/s observed at 100 RPM, but not at lower RPM.

For a well angle of 48º, the difference in cuttings bed from tests with open hole and cased hole is small. This is expected as the flow starts to get closer to vertical flow where mechanical friction between cuttings particles (cuttings bed) and wellbore becomes less important. The results show, as expected, that hole cleaning is better with higher velocity.

When the well angle increases to 60º, gravity becomes more important and a particle bed is more easily formed. Rotation of the drill string has a significant effect; especially at the lower flow velocity of 0.7 m/s shown in FIGURE 9 but still pronounced at the higher flow velocity of 0.9 m/s shown in FIGURE 10.

For the highest tested drill string rotation, 150 RPM, there are not enough cuttings bed in any of the tested cases to identify different behavior.

For the 60º inclination a test with drill string rotation at 3 RPM is included (FIGURE 9). No improvement in the hole cleaning is achieved by such low rotation. A small increase in bed height is, in fact, observed for open hole when slow rotation is applied while only a negligible change in bed height is observed in the cased configuration.

Flow rates corresponding to annular velocities like 0.7 and 0.9 m/s, as in these figures, are selected since they are among the most applied annular velocities for drilling deviated wellbores in 12 ¼" and 8 ½" sections. At higher flow rates some of the observed differences between angles, rotation and wellbore surface becomes smaller and more difficult to see.

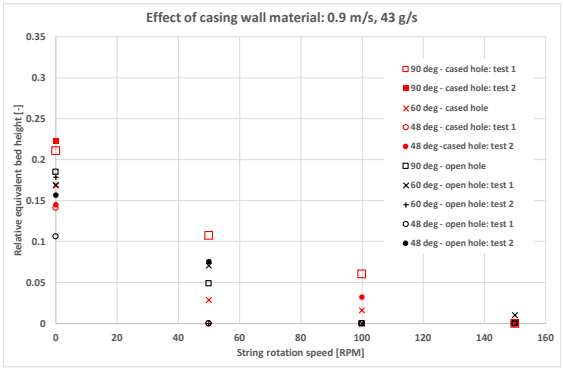

FIGURE 10. SAND BED HEIGHT FOR ANNULAR VELOCITY OF 0.9 M/S AS FUNCTION OF DRILL STRING ROTATION AT THREE INCLINATIONS FOR CASED AND OPEN HOLE CONDITIONS. SAND INJECTION RATE IS 43 G/S.

CONCLUSIONS

The main conclusion is that the wellbore wall has significant effect on pressure drop measurements and hole cleaning efficiency in highly deviated wellbores. A cased hole gives lower pressure drop while the cuttings bed height in some cases is higher. In order to model the wellbore hydraulics properly these effects must be considered.

These results also verify previous findings that hole cleaning is significantly improved if the well angle is less than a critical well deviation angle at given flow rate and drill string rotation. In these experiments such critical angle appears to be less than 60º from vertical without drill string rotation and between 60º and 90º when the drill string rotation is 50 and 100 RPM. For 150 RPM drill string rotation no, or next to no, cuttings bed is found in the test section.

The calculations performed in the present work clearly demonstrates the importance of selecting

viscosity data from the actual shear rate range. Hence, the validity of calculations using viscosity models developed in accordance with the API specifications can be questioned.

ACKNOWLEDGMENTS

The authors appreciate that Aker BP supported this work both financially and technically. The authors are also grateful that Aker BP has approved publication of these findings. The authors thank Schlumberger MI-SWACO Fluids for providing the fluids and technical support required for completing this work.

REFERENCES

[1] Sayindla, S., Lund, B., Ytrehus, J. D., and Saasen, A., 2017, "Hole-cleaning performance comparison of oil-based and water-based drilling fluids," *Journal of Petroleum Science and Engineering*, 158, pp. 49-57.

[2] Werner, B., Myrseth, V., and Saasen, A., 2017, "Viscoelastic Properties of Drilling Fluids and Their Influence on Cuttings Transport," *Journal of Petroleum Science and Engineering*, 156, pp. 845-851.

[3] Bizhani, M., and Kuru, E., 2017, "Particle Removal From Sandbed Deposits in Horizontal Annuli Using Viscoelastic Fluids," *SPE Journal*, preprint.

[4] Li, J., and Luft, B., 2014, "Overview Solids Transport Study and Application in Oil-Gas Industry-Theoretical Work," *International Petroleum Technology Conference*, International Petroleum Technology Conference, Kuala Lumpur, Malaysia.

[5] Li, J., and Luft, B., 2014, "Overview of Solids Transport Studies and Applications in Oil and Gas Industry - Experimental Work," *SPE Russian Oil and Gas Exploration & Production Technical Conference and Exhibition*, Society of Petroleum Engineers, Moscow, Russia.

[6] Busahmin, B., Saeid, N. H., Alusta, G., and Zahran, E.-S. M. M., 2017, "Review on Hole Cleaning for Horizontal Wells," *ARPN Journal of Engineering and Applied Sciences*, 12(16), pp. 4697-4708.

[7] American Petroleum Institute, 2003, "Recommend Practice for Field Testing Water-Based Drilling Fluids. API RP 13-B1, third edition."

[8] Akhshik, S., Behzad, M., and Rajabi, M., 2016, "CFD-DEM simulation of the hole cleaning process in a deviated well drilling: The effects of particle shape," Particuology, 25, pp. 72-82.

[9] Amanna, B., and Khorsand Movaghar, M. R., 2016, "Cuttings transport behavior in directional drilling using computational fluid dynamics (CFD)," *Journal of Natural Gas Science and Engineering*, 34, pp. 670-679.

[10] Ulker, E., and Sorgun, M., 2016, "Comparison of computational intelligence models for cuttings transport in horizontal and deviated wells," *Journal of Petroleum Science and Engineering*, 146, pp. 832-837.

[11] Heydari, O., Sahraei, E., and Skalle, P., 2017, "Investigating the impact of drillpipe's rotation and eccentricity on cuttings transport phenomenon in various horizontal annuluses using computational fluid dynamics (CFD)," *Journal of Petroleum Science and Engineering*, 156, pp. 801-813.

[12] Naganawa, S., Sato, R., and Ishikawa, M., 2017, "Cuttings-Transport Simulation Combined With Large-Scale-Flow-Loop Experimental Results and Logging-While-Drilling Data for Hole-Cleaning Evaluation in Directional Drilling," *SPE Drilling & Completion*, 32(3).

[13] Taghipour, A., Lund, B., Ytrehus, J. D., Skalle, P., Saasen, A., Reyes, A., and Abdollahi, J., 2014, "Experimental Study of Hydraulics and Cuttings Transport in Circular and Noncircular Wellbores," *J. Energy Resour. Technol.*, 136(2).

[14] Bolivar, N., Dear, S. F., Young, J. B., Massam, J., and Reid, T., 2007, "Field Result of Equivalent Circulating Density Reduction with a Low-Rheology Fluid," *SPE/IADC Drilling Conference*, Society of Petroleum Engineers, Amsterdam, The Netherlands.

[15] Founargiotakis, K., Kelessidis, V. C., and Maglione, R., 2008, "Laminar, transitional and turbulent flow of Herschel-Bulkley fluids in concentric annulus," *The Canadian Journal of Chemical Engineering*, 86, pp. 676-683.

[16] Haciislamoglu, M., and Langlinais, J., 1990, "Non-Newtonian flow in eccentric annuli," *Journal of Energy Resources Technology*, 112.

[17] Haciislamoglu, M., and Cartalos, U., 1994, "Practical pressure loss predictions in realistic annular geometries. Paper SPE 28304.," *69th SPE Annual Technical Conference and Exhibition*, SPE, ed.New Orleans (USA).

[18] Kelessidis, V. C., Dalamarinis, P., and Maglione, R., 2011, "Experimental study and predictions of pressure losses of fluids modeled as Herschel-Bulkley in concentric and eccentric annuli in laminar, transitional and turbulent flows," Journal of Petroleum Science and Engineering, 77, pp. 305-312.

[19] Sayindla, S., Lund, B., Ytrehus, J. D., and Saasen, A., 2017, "CFD Modelling of Observed Cuttings Transport in Oil-Based and Water-Based Drilling Fluids," SPE/IADC Drilling Conference and Exhibition, Society of Petroleum Engineers, The Hague, The Netherlands, p. 12.

[20] Ytrehus, J. D., Lund, B., Taghipour, A., Kosberg, B. R., Carazza, L., Gyland, K. R., and Saasen, A., 2018, "Cuttings Bed Removal in Deviated Wells (OMAE2018-77832)," 37th International Conference on Ocean, Offshore and Arctic Engineering, ASME, Madrid.